36
Spatial tessellations

B BOOTS

This chapter describes selected properties of a variety of planar tessellations and examines how these properties influence the use of the tessellations in GIS. Initially, properties common to all planar tessellations are presented. Regular tessellations are considered in the context of image representation and in spatial statistical analysis. Relationships frequently encountered in irregular tessellations are described. A large family of tessellations which arise as the result of data transformations is introduced. Collectively, these are known as generalised Voronoi diagrams. Their use in a variety of contexts, including solving locational problems, defining spatial relationships, and spatial interpolation is illustrated by focusing on two specific types of diagram, the ordinary Voronoi diagram and higher order Voronoi diagrams.

1 PRELIMINARIES

A tessellation of d-dimensional, Euclidean space, $\Re^d$, can be defined from two different yet equivalent perspectives. It may be considered either as a subdivision of $\Re^d$ into d-dimensional, non-overlapping regions or as a set of d-dimensional regions which cover $\Re^d$ without gaps or overlaps. These two perspectives are reflected in the use of various synonyms for tessellation, partitions, and tilings, respectively, being the most common (Grunbaum and Shephard 1986: 16). Although these two perspectives can be resolved into one by adopting a more formal definition of a tessellation, such as that given below, it is useful to maintain the distinction within the context of GIS. If a tessellation is considered as a data model, the two perspectives can be viewed as different data structures for representing the model (Peuquet 1984). The former perspective, emphasising the boundaries of the regions, is consistent with a vector structure that might be used to represent the spatial units in a choropleth map. The latter perspective, focusing on the interiors of the regions, is equivalent to a raster structure such as that formed by the pixels of a remotely-sensed image.

Tessellations have long been the subject of human interest. Indeed, the term is derived from the Latin word 'tessella', a small, square stone used to create mosaics. Despite their antiquity, new forms, such as Penrose tilings, popularly encountered in some screen savers, have only been discovered in the past 25 years (Ammann et al 1992; Grunbaum and Shephard 1986: 10 and 11). Today, tessellations are studied in a wide range of disciplines from astronomy (Zaninetti 1993) to zoology (Perry 1995). An inevitable, but unfortunate, consequence of this widespread use is that many characteristics of tessellations and their component parts are known by a variety of names. Consequently, it is necessary to begin by defining a number of terms. As far as possible usage is consistent with current GIS practice.

To begin with a formal definition of a tessellation: Let S be a closed subset of $\Re^d$, $\Im = \{s_1,...,s_n\}$ where s_i is a closed subset of S, and s_i' the interior of s_i. If the elements of $\Im$ satisfy

$$s_i' \cap s_j' = \emptyset \text{ for } i \neq j \tag{1}$$

$$\bigcup_{i=1}^{n} s_i = S, \tag{2}$$

then the set $\Im$ is called a tessellation of S. Property (1) means that the interiors of the elements of $\Im$ are disjoint and (2) means that collectively the elements of $\Im$ fill the space S. Note that this definition is consistent

with practical applications such as those encountered in GIS, where the space under consideration is a bounded region in Euclidean space rather than the unbounded space itself (the usual situation in theoretical treatments). When d=2 the tessellation is called a *planar tessellation*. Attention in this chapter is limited to planar tessellations since these are those most commonly encountered in GIS.

Planar tessellations are composed of three elements of d ($d \leq 2$) dimensions (see Figure 1): cells (2-d), edges (1-d), and vertices (0-d). In GIS these elements are usually referred to as polygons, lines (or arcs), and points respectively. In turn, each of the d (d>0)-dimensional elements are composed of elements of (d-1) dimensions. Cells have sides (1-d) and corners (0-d), lines have end points (0-d). A tessellation, such as that in Figure 1, in which the corners and sides of individual cells coincide with the vertices and edges of the tessellation, respectively, is called an *edge-to-edge tessellation*. Individual rectangular cells arranged in a brick wall fashion would not constitute an edge-to-edge tessellation. Only edge-to-edge tessellations are considered here. A d-dimensional tessellation in which every s-dimensional element lies in the boundaries of (d–s+1) cells ($0 \leq s \leq d-1$) is called a *normal tessellation*. Thus, in a normal planar tessellation, each vertex is shared by three cells and each edge is common to two cells.

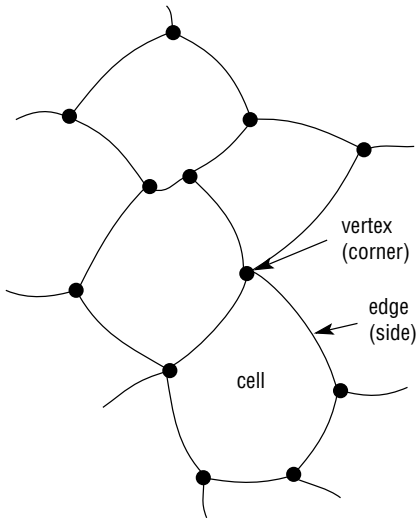

Fig 1. Illustration of terms for tessellations and cells (in parentheses).

A *monohedral tessellation* is one in which all the cells are of the same size and shape (e.g. the tessellation in Figure 2). More formally, each cell is congruent (directly or reflectively) to one fixed set S. If r_i denotes the number of edges meeting at the ith corner of a cell in a monohedral tessellation, an *isohedral tessellation* is one in which the ordered sequence of values of r_i is the same for every cell. In short, the cells are completely interchangeable so that, as Bell and Holroyd (1991) note, 'a bug which was put down in one of the [cells] and started to explore the [tessellation] would find exactly the same arrangement of [cells] no matter which [cell] it was originally deposited in'. More formally, all the cells are equivalent under the symmetry group of the tessellation. Thus, the tessellation in Figure 3 is isohedral while that in Figure 2 is not.

A regular polygon is one with equal side length and equal internal angles. Grunbaum and Shephard (1977a) demonstrate that, even if we restrict our attention to tessellations consisting of only one type of regular polygon, the number of such tessellations is infinite. However, by imposing the condition that all the vertices of the tessellation are of the same type, the number reduces dramatically to just 11. These are the so-called *Archimedean tessellations* (see Figure 4), also known as *uniform tessellations.*

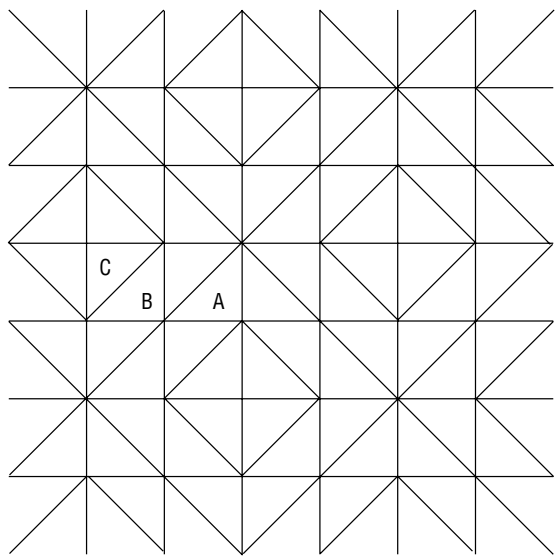

Fig 2. A monohedral tessellation containing three types of cells A, B, and C, each of the same size and shape but arranged differently.

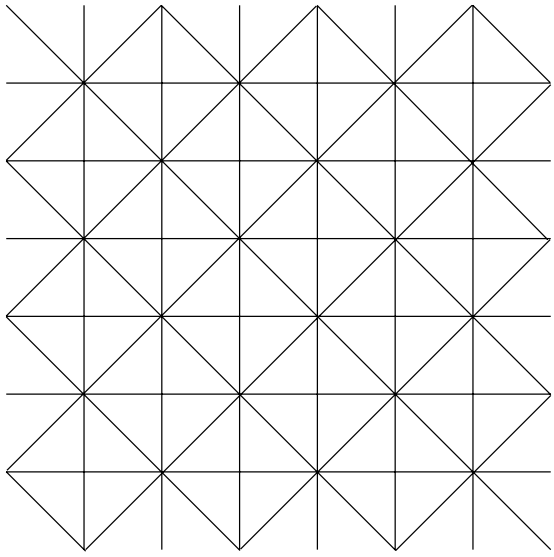

Fig 3. An isohedral tessellation in which all cells are of the same size and shape and are arranged identically.

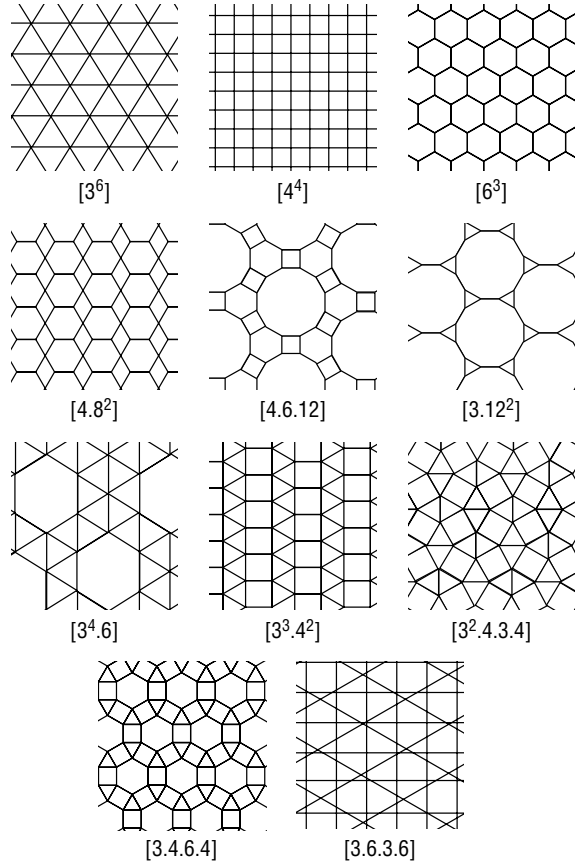

Fig 4. The 11 distinct Archimedean (uniform) tessellations.

The three uniform tessellations which are also isohedral (i.e. those consisting of regular triangles, squares, or hexagons) are called *regular tessellations*.

If there is a one-to-one correspondence between the vertices, edges, and cells of one tessellation and the cells, edges, and vertices of another tessellation, the two tessellations are called each other's *dual tessellation* (see Figure 5). A dual tessellation can be generated from a tessellation T in the following way. Select a point q_i in each cell c_i of T. For each pair of cells c_i, c_j which share an edge of T, construct a line segment joining q_i, q_j. Because there is no unique way of selecting q_i, it is possible to generate more than one metric dual.

A d-dimensional tessellation consisting exclusively of cells with $(d+1)$ sides is called a *simplex* (or simplicial graph). The dual tessellation in Figure 5 is a simplex since all its cells are triangles. Another example is the triangulated irregular network (TIN) often encountered in GIS to represent continuous surfaces (Hutchinson and Gallant, Chapter 9).

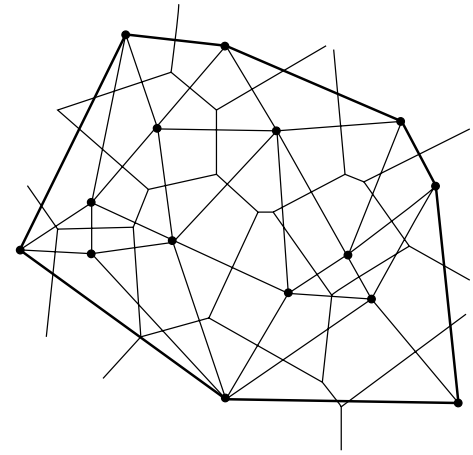

Fig 5. A tessellation (heavier lines) and a dual tessellation (lighter lines).

2 GENERAL PROPERTIES

Here we present properties which hold for all tessellations satisfying a specific condition known as the closure postulate. This postulate requires that at

least two edges meet at every vertex and at least two cells meet at every edge. The elements in such tessellations are related to each other through Equation 3 derived by Schlaefli in 1852 as a generalisation of a relationship first formulated by Euler one hundred years earlier (Loeb 1976):

$$\sum_{i=0}^{j} (-1)^i N_i = 1 + (-1)^j \quad (3)$$

where N_i is the number of elements of dimensionality i. For planar tessellations Equation 3 reduces to:

$$N_0 - N_1 + N_2 = 2 \quad (4)$$

where N_0, N_1, N_2 are the number of vertices, edges, and cells respectively. To satisfy the closure postulate, if our tessellation is bounded, we must include in our count of N_2 an outside cell whose number of sides is equal to the number of edges on the boundary of the tessellation.

If we define r=number of edges meeting at a vertex and n=number of corners or sides of a cell, a further equation can be derived from Equation 4, which reveals that we need only three parameters to specify all of the characteristics of the tessellation. This equation is

$$1/\bar{r} - 1/2 + 1/\bar{n} = 1/N_1 \quad (5)$$

where $\bar{r}$ and $\bar{n}$ are the mean values of r and n, respectively. Equation 3 yields expressions for

$$N_0 = 2N_1/\bar{r} \quad (6)$$

and

$$N_2 = 2N_1/\bar{n} \quad (7)$$

The verification of Equations 3–7 is left as an exercise for the reader.

3 REGULAR TESSELLATIONS

This and the next section continue the exploration of properties of tessellations by looking in more detail at specific types of tessellations. However, the emphasis is shifted away from the properties themselves towards an examination of how they might influence the use of the tessellations within specific contexts in GIS. The first example involves the use of tessellations as spatial data models, in particular in image representation.

To be useful in such a role tessellations should ideally possess at least two properties (Ahuja 1983; Samet 1989):

1. be capable of generating an infinitely repetitive pattern, so that they can be used for images of any size;
2. be infinitely (recursively) decomposable into increasingly finer patterns which, collectively, form a hierarchy, to allow for the representation of spatial features of arbitrarily fine resolution.

If attention is restricted to tessellations consisting of only one type of cell, a reasonable starting point is to consider isohedral tessellations, particularly since Grunbaum and Shephard (1977b) demonstrate that there are only 81 such planar tessellations. This number further reduces to 11 if only those tessellations are considered which are topologically distinct (i.e. all edges in the 81 tessellations are straight lines). These 11 (see Figure 6) are known as

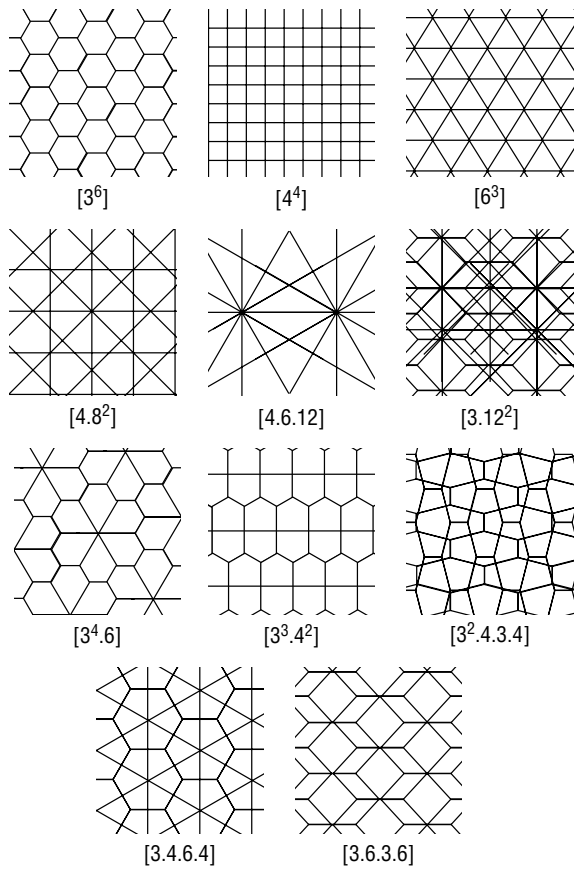

Fig 6. Laves tessellations.

Laves tessellations after the famous crystallographer Fritz Laves. Laves tessellations may also be derived as duals of the uniform (Archimedean) tessellations in Figure 4. Note that three of the Laves tessellations are regular tessellations. To describe Laves tessellations we use a notation based on the number of edges at the vertices of a constituent cell as they are visited in cyclic order (see Figure 6). Thus, the three regular tessellations consisting of triangles, squares, and hexagons are labelled [6^3], [4^4] and [3^6] respectively.

Before pursuing the second property, some additional definitions are required. An *atomic polygon* is an individual cell in a tessellation at the lowest level k (k=0) in a hierarchy of tessellations. A *molecular polygon* is an aggregate of atomic polygons used in forming the higher levels (k>0) of a hierarchy. The molecular polygon need not be the same shape as the atomic polygon. When the cells at level k of a hierarchy have the same shape as those at level (k+1), the tessellation is said to be unlimited. Alternatively, we can think of unlimited tessellations as lacking a definable atomic polygon since any cell can always be subdivided into cells of the same shape.

The second property suggests that we require unlimited tessellations. Of the 11 Laves nets, only four are unlimited (Bell et al 1983). Two of these are regular tessellations, [6^3] and [4^4], each of which are capable of generating an infinite number of different molecular tessellations where each first level molecular polygon consists of $s=n^2$ (n>1) atomic polygons (see Figure 7). The other two unlimited tessellations are [4.8^2] and [4.6.12], each of which gives rise to two types of hierarchy: [4.8^2] has an ordinary ($s=n^2$, n>1) and a rotation (135 degrees between levels) hierarchy ($s=2n^2$, n>1); while [4.6.12] has an ordinary and a reflection hierarchy ($s=3n^2$, n>1) (see Figure 7).

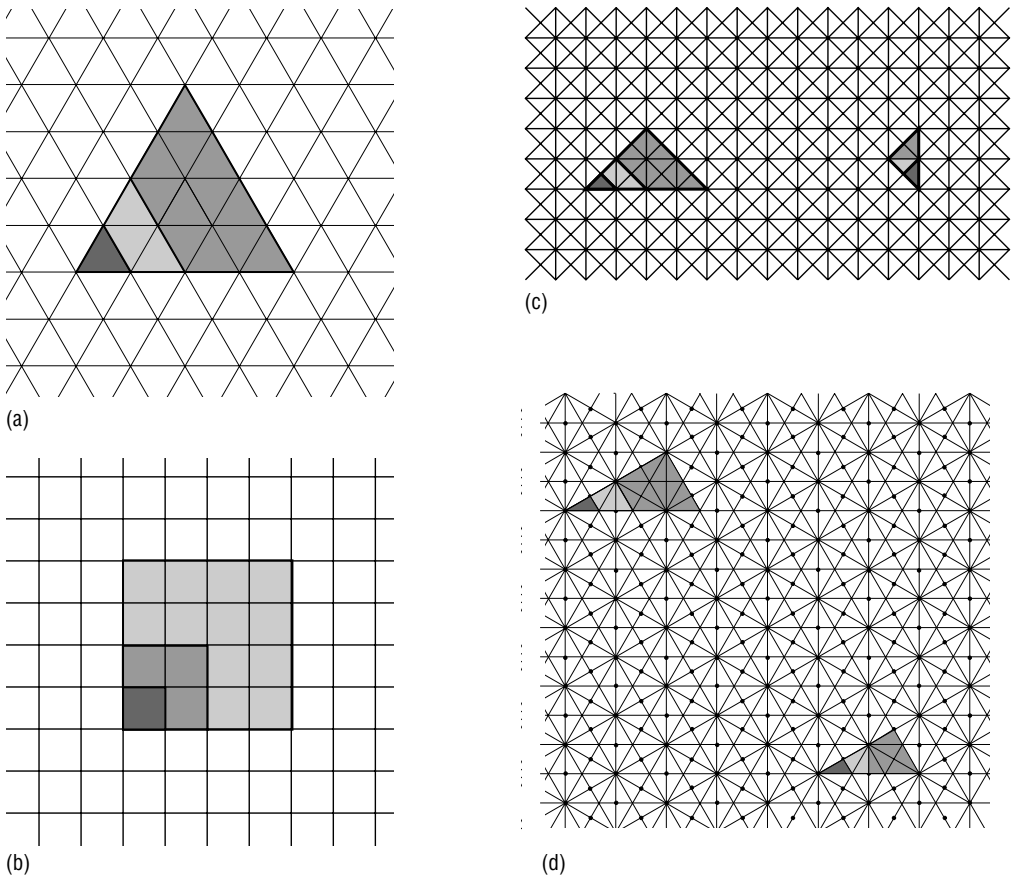

Fig 7. Unlimited tessellations (a) [6^3]; (b) [4^4]; (c) [4.8^2], ordinary hierarchy (left-hand side), rotation hierarchy (right-hand side); (d) [4.6.12], ordinary hierarchy (left-hand side), reflection hierarchy (right-hand side).

Bell et al (1983, 1989) suggest additional tessellation properties which are valuable in image processing and automated cartography applications. Of these, the two most important are uniform adjacency, whereby the distances between the centroid of a given cell and those of neighbouring cells (whether edge or vertex neighbours) are the same, and uniform orientation which means that all cells have the same orientation. However, none of the four unlimited tessellations possess the first property; [4^4] has two adjacency distances, [6^3] three, [4.8^2] eight, and [4.6.12] 16. Further, only [4^4] displays uniform orientation. This situation leads to a reconsideration of the remaining regular tessellation [3^6] which possesses both properties even though it is not unlimited.

Although [3^6] cannot be decomposed beyond the atomic tessellation without changing the shape of the cell, by defining molecular polygons made up of different numbers of atomic hexagons, it is possible to generate a large number of hexagonal hierarchies. While such hierarchies can always be grouped upwards, they cannot necessarily be decomposed downwards. These molecular polygons are referred to as n-*shapes*. More than one *n*-shape is possible for a given value of *n* (see Figure 8) and by using different rotations, the same molecular cell can give rise to more than one hierarchy (Diaz 1986) (compare the 'propeller' in Figure 8(b) with the 'wombat' in Figure 8(c)).

The *n*-shape which has received most attention is the 7-shape whose form most closely resembles that of the atomic hexagon (see Figure 9). Unfortunately, as Figure 9 shows, each level of the hierarchy formed by this 7-shape is rotated by an irrational angle with respect to the previous one.

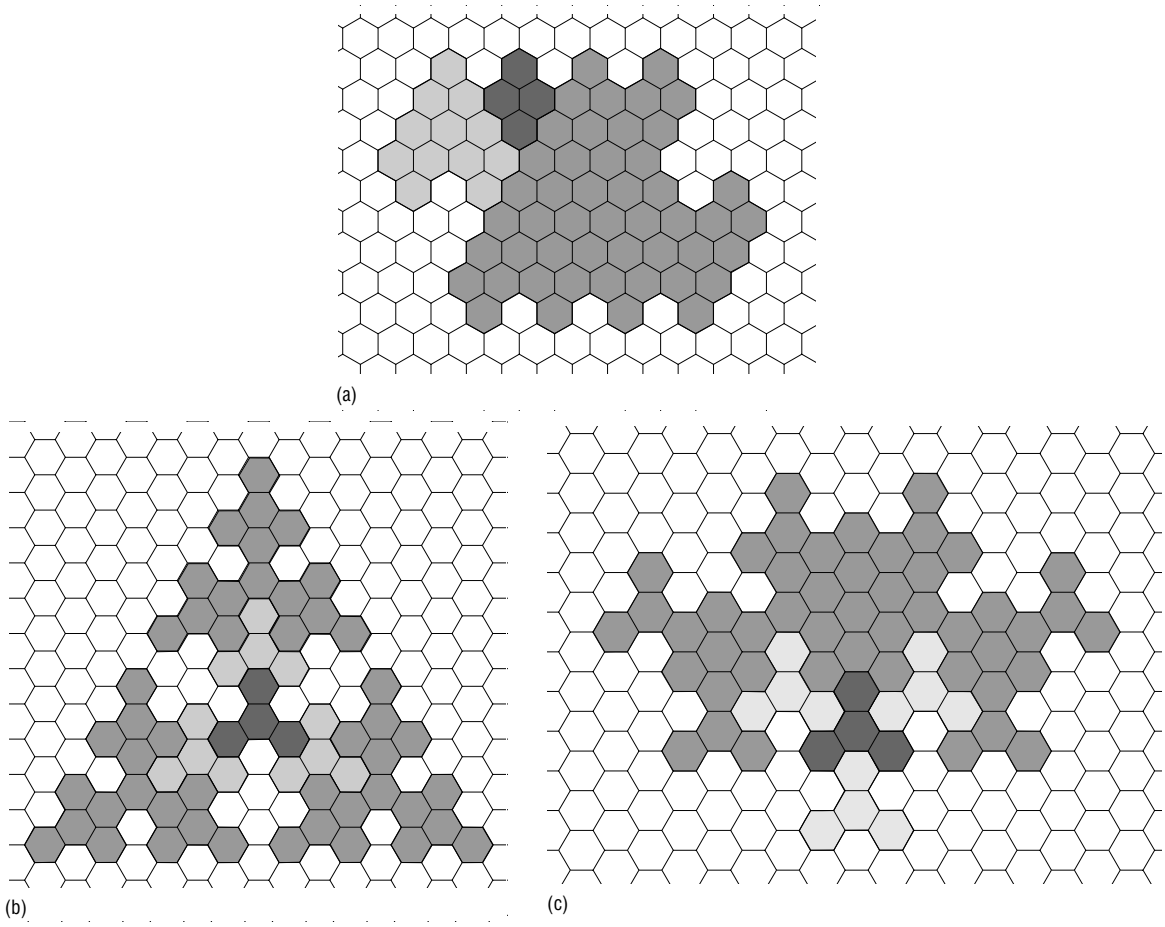

Fig 8. Three different hexagonal hierarchies using 4-shapes.

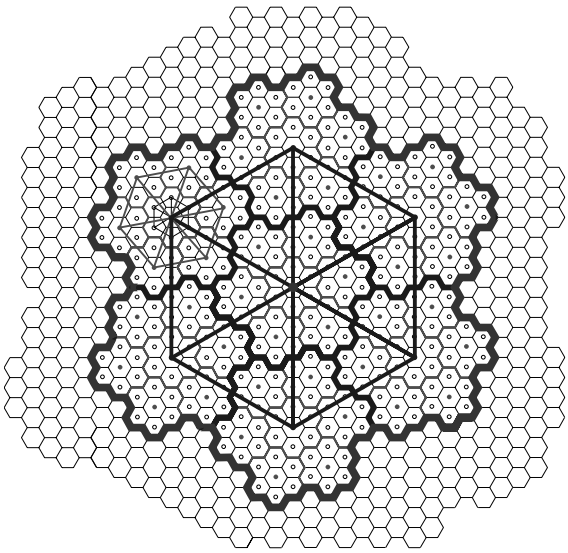

Fig 9. Hexagonal hierarchy using a 7-shape.

Even though the cells of a hexagonal tessellation are not infinitely recursively decomposable, by representing each hexagonal cell by its centroid, a triangular lattice is formed in which it is possible to embed similar (triangular), finer grids (Holroyd and Bell 1992) (e.g. the lattices formed by the cell centroids in Figure 9). Recognising this, Bell et al (1989) propose a compromise between [4^4] and [3^6] by presenting a point lattice over which both a hexagonal and a rhombic (4-edge) tessellation can be placed (see Figure 10). At the lowest hierarchical level, the lattice points are simultaneously the vertices of the rhombic tessellation and the centroids of the hexagonal tessellation. The rhombic lattice has the same properties as [4^4] in terms of adjacency and unlimitedness while the hexagonal tessellation can be amalgamated by a 4-shape which is only limited at the atomic level and which, unlike the 7-shape hexagonal tessellation described above, also maintains the same orientation for molecular cells at all levels. Bell et al (1989) call this the hexagonal or rhombic (HoR) tessellation. Despite providing an addressing system for HoR and showing that it has advantages over the addressing system for the 7-shape, they do not appear to have been successful in persuading others to adopt it.

As another illustration of how the properties of regular tessellations influence their use in GIS,

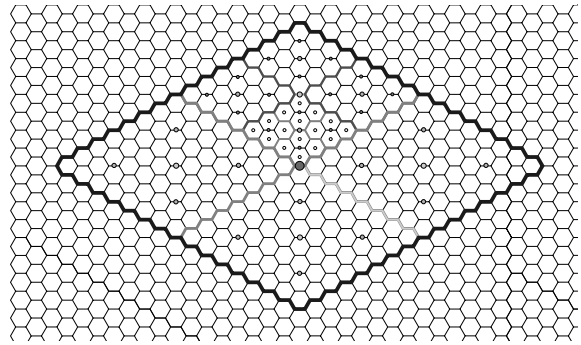

Fig 10. Hexagonal or rhombic (HoR) tessellation.

consider a situation from spatial statistical analysis. Recently, there has been considerable interest in integrating spatial data analysis in GIS (see Anselin, Chapter 17; Church, Chapter 20; Fischer, Chapter 19; Getis, Chapter 16; Openshaw and Alvanides, Chapter 18; Ding and Fotheringham 1992; Fotherigham and Rogerson 1993; Goodchild et al 1992). One measure used extensively in spatial analysis which is already incorporated in many GIS is spatial autocorrelation. Although spatial autocorrelation has numerous uses in spatial data analysis (Griffith 1992), one of the most fundamental is as an indicator of the spatial pattern exhibited by the values of a variable x recorded at a set of observations (cells, in the case of tessellations) located in space. The most frequently used measure of spatial autocorrelation is Moran's I given by Equation 8:

$$I = (n / \sum_i \sum_j d_{ij}) [\sum_i \sum_j d_{ij} (x_i - \bar{x}) (x_j - \bar{x}) / \sum_i (x_i - \bar{x})^2] \quad (8)$$

where n is the number of cells, d_{ij} is a measure of the spatial relationship between cells i and j, x_i is the value of variable x for cell i, and $\bar{x}$ is the mean value of x.

The expected value of I is $E(I) = -[1/(n-1)]$. Positive spatial autocorrelation, $I > E(I)$, occurs when similar values of x are found in spatial juxtaposition while negative spatial autocorrelation, $I < E(I)$, occurs when neighbouring values of x are dissimilar. Since this statistic incorporates a measure of the spatial association between pairs of cells in the tessellation, the calculated value of I reflects the underlying geometry of the tessellation as well as the values of the variable x. In particular, Jong et al (1984) show that the tessellation geometry imposes limits on the feasible values of I. To demonstrate this, first consider an

alternative graph theory representation of a tessellation. This involves defining a binary connectivity matrix, **C,** whose elements c_{ij}=1 if cells *i* and *j* have a common edge, and 0, otherwise (by definition c_{ii}=0). Jong et al (1984) demonstrate that the maximum and minimum values of *I* can be obtained from the largest and smallest eigenvalues of the matrix

$$\mathbf{MCM} = (\mathbf{I}-\mathbf{11}^T/n)\,\mathbf{C}(\mathbf{I}-\mathbf{11}^T/n) \qquad (9)$$

The limits on *I* are investigated here for the three regular tessellations. Since the geometry of a bounded tessellation is not independent of the number of cells *n* in the tessellation (e.g. as *n* increases, the proportion of boundary cells decreases), tessellations of three different sizes (*n*=64, 256, 1024) are examined.

Table 1 shows a number of ways in which the limits on *I* are influenced by the geometry of the tessellation. First, for any given regular tessellation, the range of feasible values of *I* changes as *n* changes. Second, for any given value of *n*, the limits for the tessellations of squares and triangles are quite similar and, further, this similarity increases as *n* increases. Third, the absolute values for the upper and lower limits for the tessellations of squares and triangles are approximately equal, indicating that similar magnitudes of spatial autocorrelation of both a positive and negative kind can occur. In contrast, for a tessellation of hexagons, extreme positive spatial autocorrelation is approximately twice the magnitude of extreme negative spatial autocorrelation. Clearly, these results suggest that caution should be exercised when interpreting differences in values of *I* obtained from spatial patterns observed in different tessellations, and that such differences should not be ascribed solely to different spatial characteristics of the variable(s) being studied.

Further results with relevance for GIS can be derived from **C**. Griffith (1996) shows that the eigenvectors of **MCM** identify the possible mutually exclusive geographical patterns of attribute values with levels of spatial autocorrelation equal in magnitude to the associated eigenvalues. To illustrate this, the three regular tessellations for the three sizes considered above are used. The geographical patterns of spatial autocorrelation remain essentially the same for a given tessellation as *n* changes. For example, Figure 11 shows the spatial patterns of the first nine eigenvectors of **MCM** for a tessellation of squares. Note that numerical eigenvectors are unique to a multiplicative factor of -1 so that patterns such as those for the third eigenvectors for *n*=256 and *n*=1024 are considered identical even though they are mirror images of each other. Also note that the pattern for eigenvector 1 for *n*=64 is the same as that for eigenvector 2 for *n*=256, while eigenvector 2 for *n*=64 is the same as that for eigenvector 1 for *n*=256 (the same also holds for the eighth and ninth eigenvectors of the two tessellations). This arises because the order of the two eigenvectors is arbitrary since they have the same associated eigenvalue. However, observe that different patterns result for different tessellations. Compare the patterns in Figures 12 and 13 for *n*=1024 for tessellations of triangles and hexagons with the corresponding patterns for the tessellation of squares in Figure 11(c). Only the pattern for the first eigenvector of **MCM** is the same for all three tessellations. Some patterns, such as that displayed by the fourth eigenvector for the tessellation of squares, are unique. Thus, all patterns of spatial autocorrelation are not equally likely to occur for all regular tessellations.

Table 1 Limits on the value of Moran's *I* for regular tessellations.

n	*Squares*	*Triangles*	*Hexagons*
64	-1.0739 0.9747	-1.0725 1.0330	-0.5519 1.0065
256	-1.0485 1.0216	-1.0477 1.0375	-0.5330 1.0403
1024	-1.0276 1.0206	-1.0273 1.0247	-0.5186 1.0306

4 IRREGULAR TESSELLATIONS

Many tessellations encountered in GIS, such as those formed by the spatial units of a choropleth map, are highly variable in terms of the characteristics of their constituent cells. Consequently, we might anticipate that it would not be possible to identify any properties of such tessellations beyond the general ones described in Section 2. However, empirical investigation has revealed that two linear relationships hold for a typical (i.e. randomly selected) *n*-sided cell in many irregular, normal tessellations consisting of only

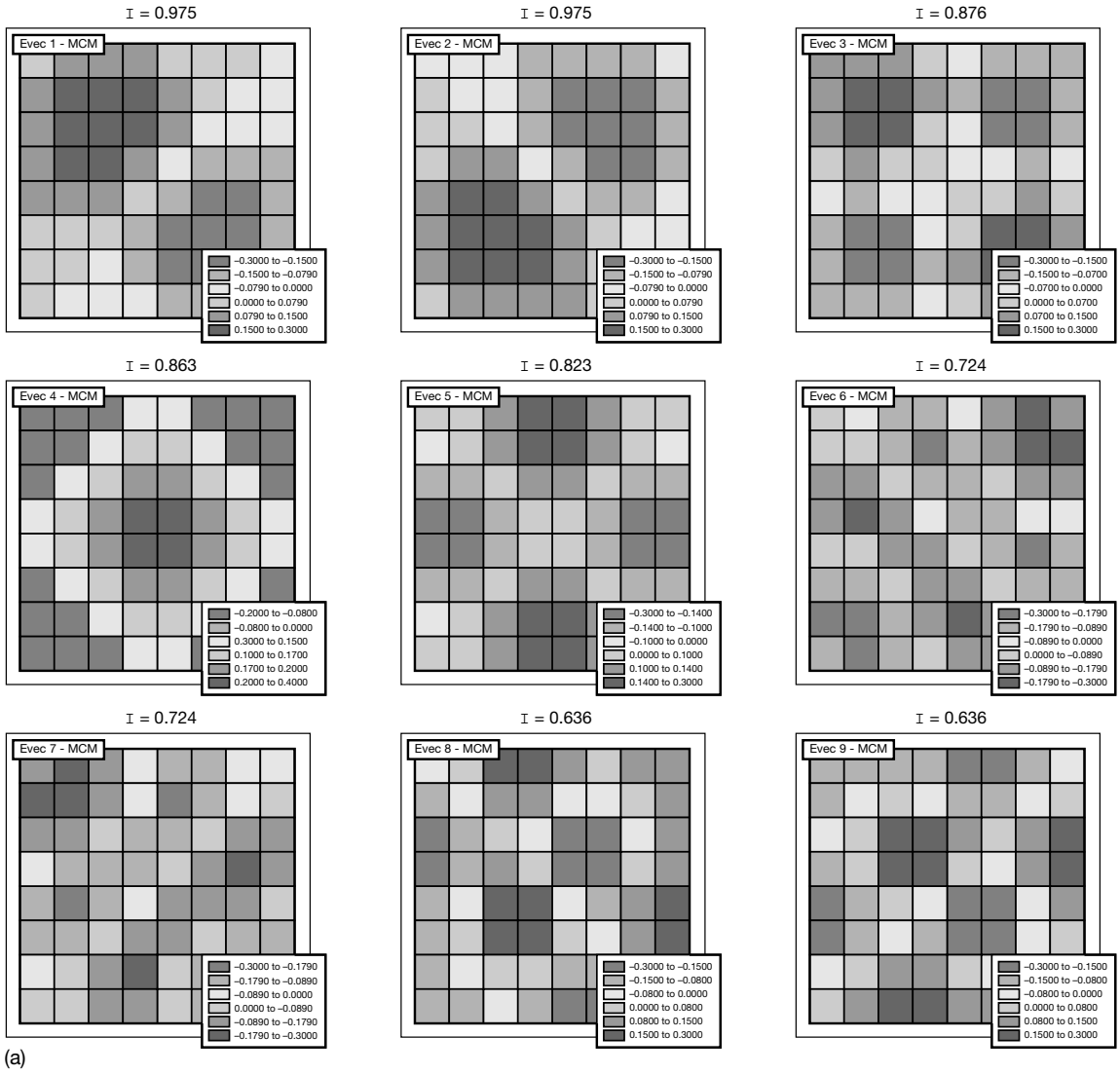

Fig 11. Spatial patterns of the elements of the first 9 eigenvectors of MCM for a tessellation of squares: (a) *n*=64; (b) *n*=256; and (c) *n*=1024. (Continued on pages 512–13)

convex cells. Because of their extensive occurrence, these relationships are usually referred to as 'laws'.

The first is *Lewis' law*, so named because the relationship was first observed by Lewis (1928, 1930, 1931, 1943, 1944) in empirical studies of a variety of biological tessellations. Lewis' law states that the average area of a typical *n*-sided cell increases with *n* in a linear fashion as described by Equation 10:

$$\bar{A}_n = (A_0 / C) + b(A_0 / C)\,(n–6) \qquad (10)$$

where $\bar{A}_n$ = average area of a *n*-sided cell; A_0 = total area of the tessellation; C = number of cells in the tessellation; and b = a constant.

The other is *Aboav's law*, in recognition that it was first observed by Aboav (1970) in studies of various polycrystalline materials. This law states that the total number of sides of the cells neighbouring a typical *n*-sided cell is linear in *n* as described in Equation 11:

$$nm_n = (6a+\mu_2) + (\bar{n} - a)\,n \qquad (11)$$

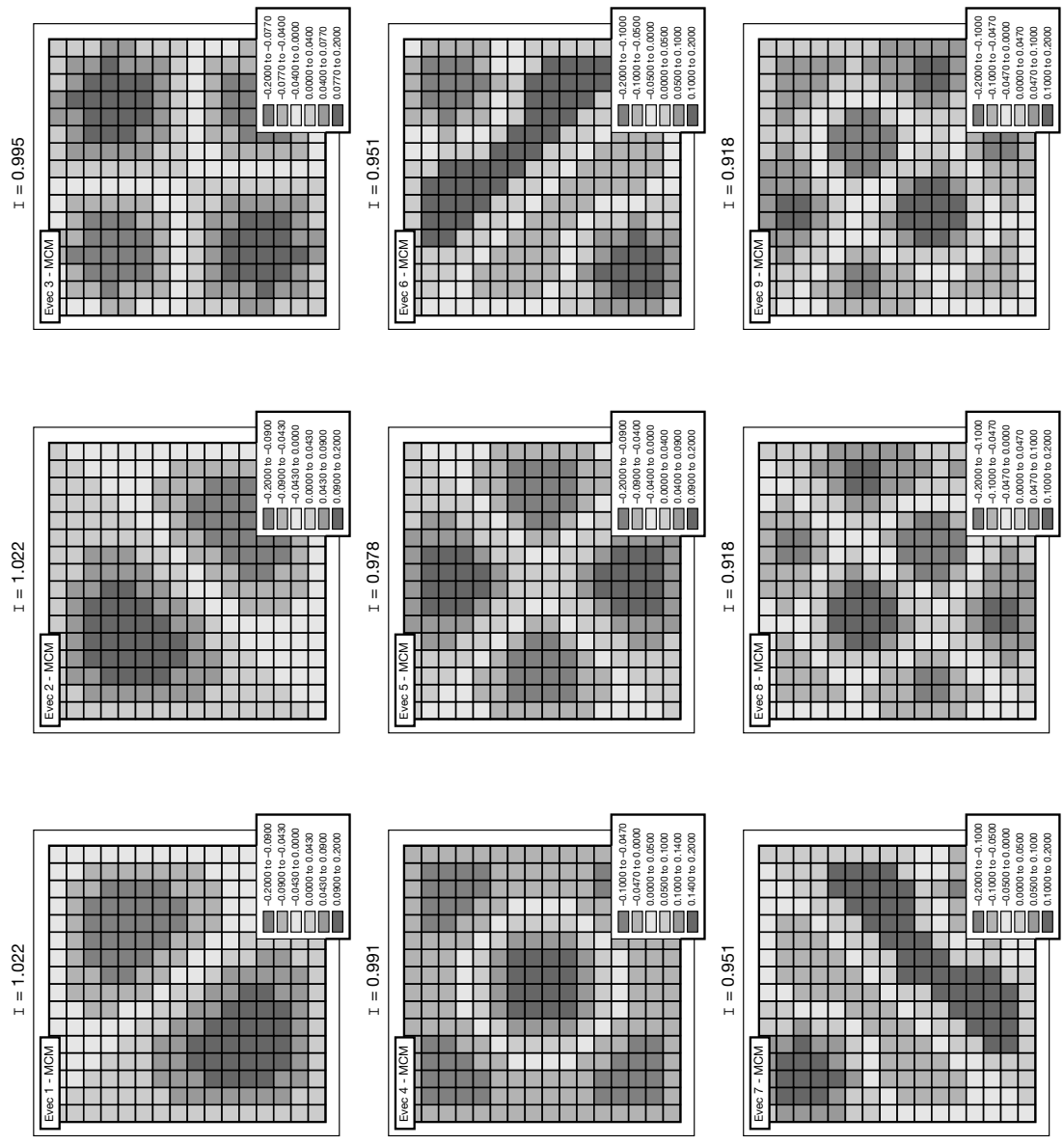

(b)

Fig 11. (continued)

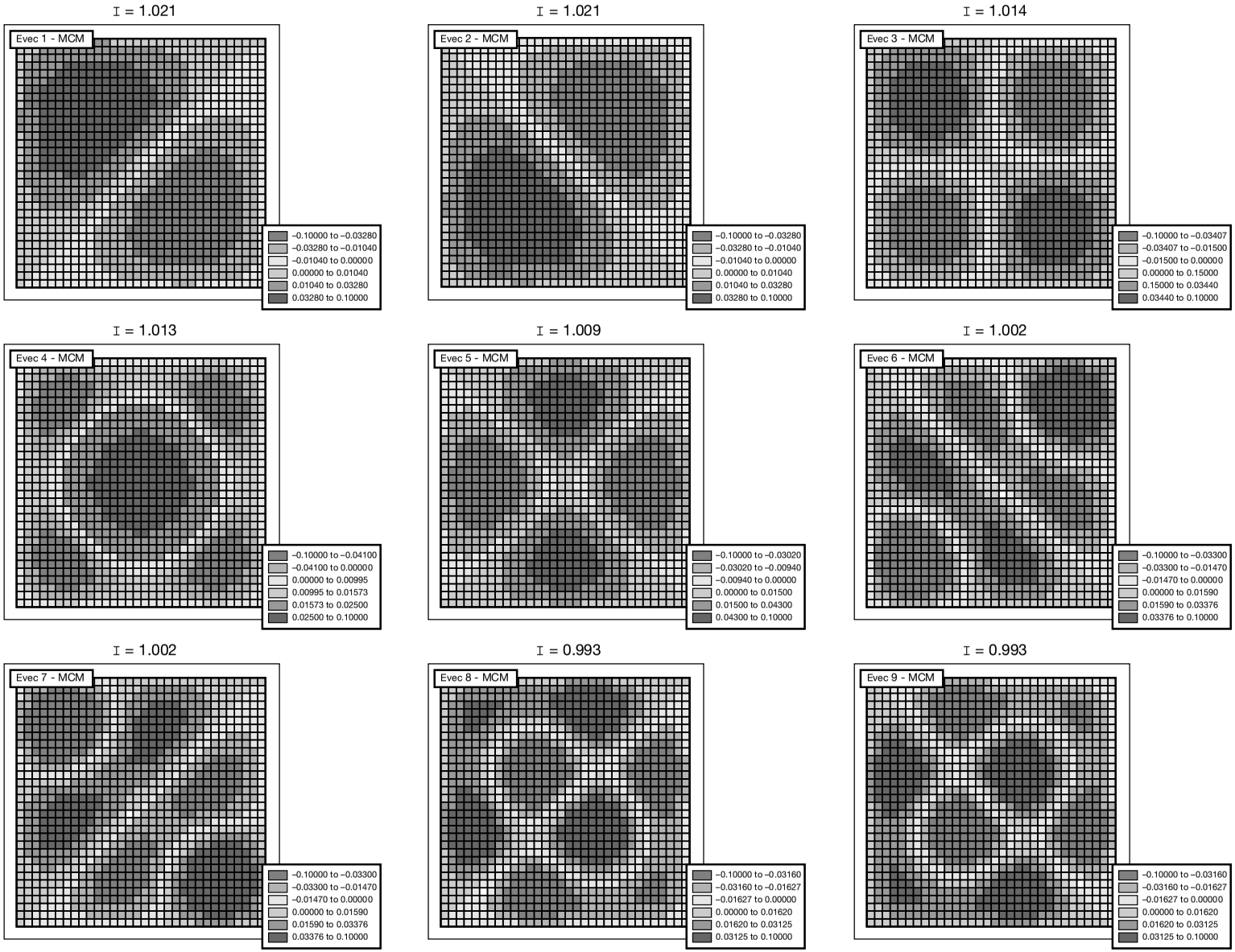

(c)

Fig 11. (continued)

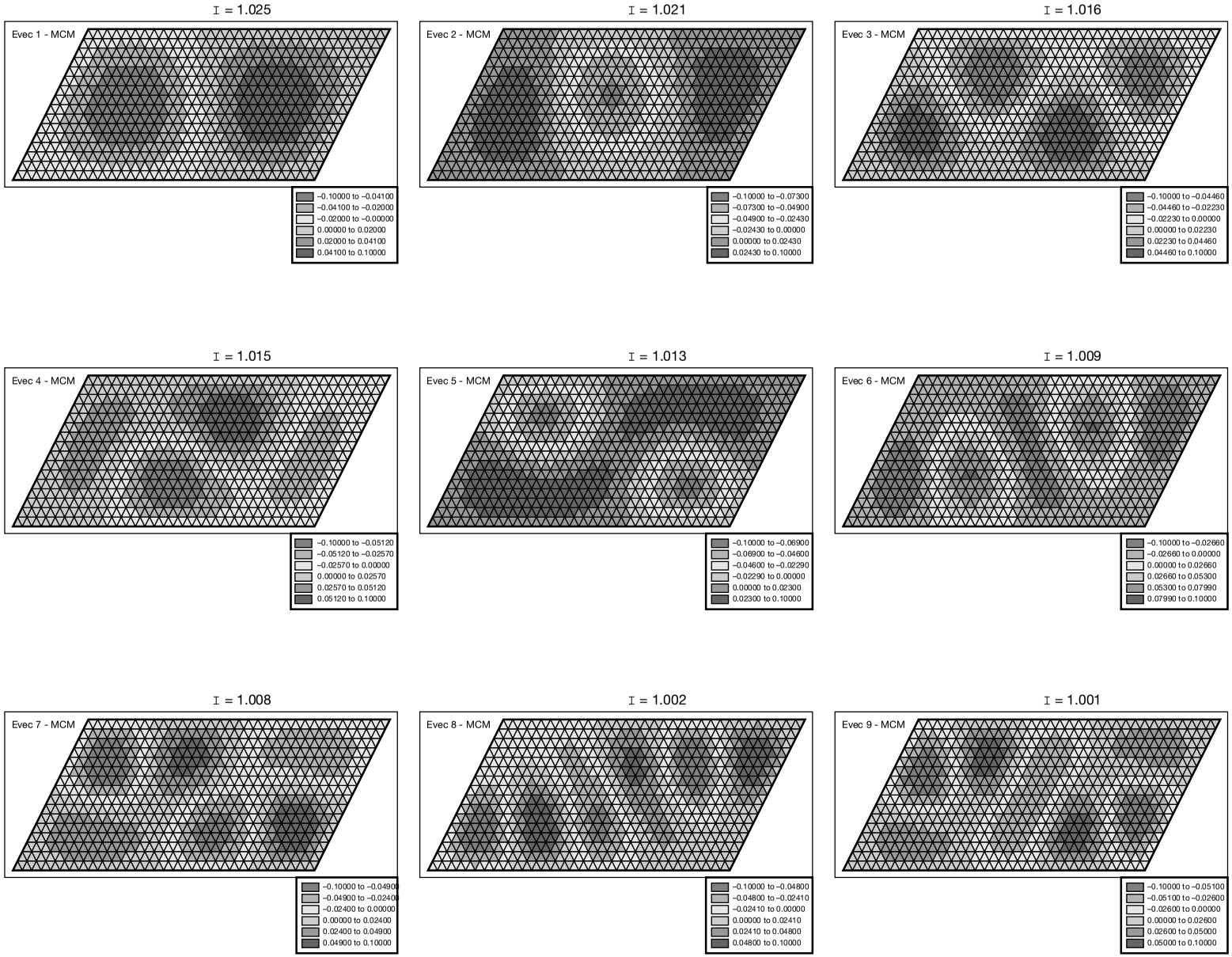

Fig 12. Spatial patterns of the elements of the first 9 eigenvectors of MCM for a tessellation of triangles, n=1024.

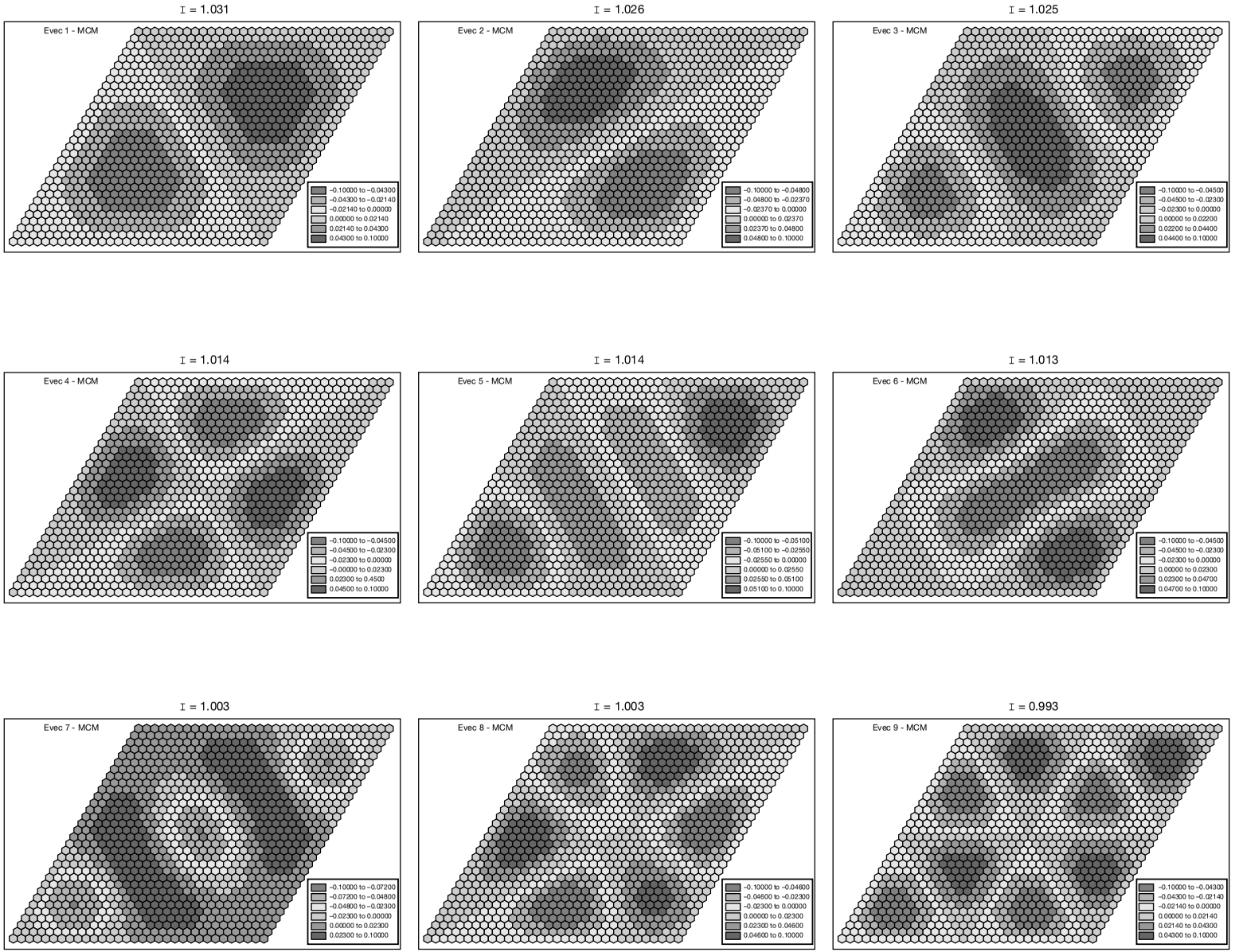

Fig 13. Spatial patterns of the elements of the first 9 eigenvectors of MCM for a tessellation of hexagons, n=1024.

where m_n = number of sides of a randomly chosen neighbour of a typical n-sided cell; $\overline{n}$ = mean value of n for the tessellation;
$\mu_2 = \overline{n^2} - (\overline{n})^2$;
$\overline{n^2}$ = mean value of n^2 for the tessellation.

This law implies that, on average, cells with few sides are likely to be adjacent to those with many sides, and vice versa.

No satisfactory explanations for the laws have yet been found. Most arguments involve an approach which maximises the entropy of p_n, the distribution of n for the tessellation, subject to a minimal set of constraints (Chiu 1995; Peshkin et al 1991; Rivier 1985, 1986, 1990, 1991, 1993, 1994; Rivier and Lissowski 1982). Both laws are seen as the most likely relationships to arise by chance in the absence of any other constraints.

Given that many kinds of tessellation encountered in GIS (e.g. politico-administrative units at all spatial scales) are likely to contain non-convex cells and may have non-trivalent vertices, it might be anticipated that neither law has much relevance to GIS. However, this conclusion would be incorrect. To illustrate this, consider the counties of the states of the USA. To avoid departing completely from the conditions specified in the laws, states with less than 25 'internal' counties or with more than 10 non-trivalent vertices are not considered. 'Internal' counties are those for which none of the sides are part of the state boundary (including coastlines). These restrictions result in 24 states being examined (see Table 2). Somewhat surprisingly, the counties of 18 states are consistent with either Lewis' law or Aboav's law, while both laws hold for eight states (see Table 2). Figure 14 shows a weighted least squares (WLS) fit of Lewis' law to the data for Pennsylvania (see Table 3), while Figure 15 shows a similar WLS fit of Aboav's law for Georgia (see also Table 4). Both laws also hold for both the 94 interior departments and 222 interior arrondissements of France (Le Caer and Delannay 1993), while Aboav's law holds for the interior administrative subdivisions of Indian states (Boots 1979), parishes of counties in southwest England (Boots 1980), and parishes of Lorraine, France (Pignol et al 1993).

What are the implications of these findings for GIS? The most obvious is that, because of the geometric constraints imposed on the 2-dimensional tessellations, there is more order present in irregular tessellations than might be suspected and that other laws may well await discovery. In terms of sampling tessellations for statistical analysis, in order to derive a sample of independent cells, it will be necessary to ensure that cells which are neighbours are not chosen. The findings also have implications for local data structures, storage, and revision.

Table 2 The incidence of Lewis' law and Aboav's law for counties of selected states in the USA.

State	*Lewis' law*	*Aboav's law*
Alabama	*	
Arkansas		*
California		
Colorado	*	*
Georgia	*	*
Illinois	*	*
Indiana	*	*
Kentucky		
Louisiana	*	*
Minnesota		
Mississippi		*
Missouri	*	
Montana	*	*
New York	*	
N. Carolina	*	*
N. Dakota		*
Ohio		*
Oklahoma	*	
Pennsylvania		*
S. Dakota		
Tennessee	*	*
Virginia	*	
W. Virginia		
Wisconsin		

Table 3 Lewis' law for the counties of Georgia, USA.

n	*f(n)*	$\overline{A}_n{}^*$
4	10	0.711
5	32	0.752
6	35	1.030
7	24	1.253
8	6	1.375
9	1	1.093
10	1	1.540

$\overline{A}_n{}^* = \overline{A}_n / (A_0 / C)$

For definition of symbols, see text.

Table 4 Aboav's law for the countries of Pennsylvania, USA.

n	*f(n)*	*nmn*
3	1	23.000
4	2	25.714
5	15	30.588
6	11	37.200
7	5	38.652
8	3	47.304
9	1	51.000

For definition of symbols, see text.

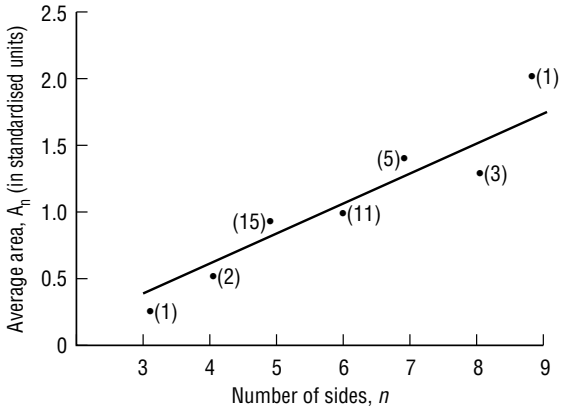

Fig 14. Weighted least squares fit of Lewis' law to the counties of Pennsylvania. Values in brackets are the number of observations used to calculate the mean value.

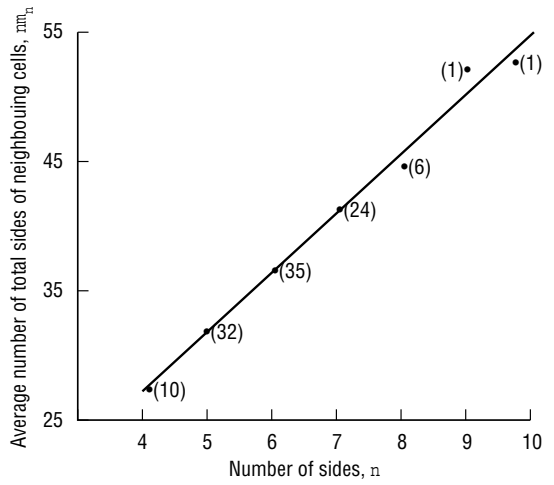

Fig 15. Weighted least squares fit of Aboav's law to the counties of Georgia. Values in brackets are the number of observations used to calculate the mean value.

5 GENERALISED VORONOI DIAGRAMS

As well as occurring directly, tessellations can also arise from data transformations performed in GIS. One such transformation involves an operation which parallels that used to create a dual tessellation (see section 1) and gives rise to a large family of tessellations known collectively as *generalised Voronoi diagrams* (GVDs). In two dimensions such tessellations can be created for any set of *s*-dimensional ($s \leq 2$) geometric entities (generators) in the plane such as points, line segments, arcs or polygons, or any combination of such elements, by assigning each location in the plane to the 'nearest' generator (Figure 16). By using different distance metrics, different definitions of nearest are possible. The presence of obstacles (non-generator, *s*-dimensional ($s \leq 2$) entities) can also

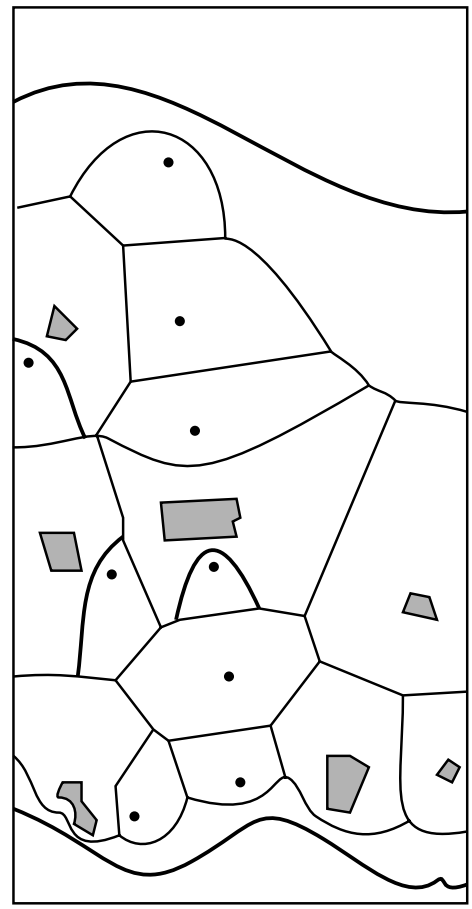

Fig 16. Voronoi diagram of points (stations), lines (rivers), and polygons (parks) in part of the Sumida-Kohto district of Tokyo.

be accommodated. By nature of their construction GVDs are necessarily edge-to-edge tessellations. Note that the three regular tessellations (square, triangle, hexagon) described in Section 1 can be generated by defining the Voronoi diagram of a set of points located on a square, hexagonal, and triangular lattice, respectively (see Figure 17). Conceptualised in this way, regular tessellations can be thought of as representing both area and point information simultaneously (Gold 1990).

GVDs are particularly useful for performing a variety of nearest neighbour operations which address locational issues arising in spatial analysis and planning, including solving continuous location problems of both location-allocation and locational optimisation kinds (Okabe et al 1994; Okabe and Suzuki 1995). In addition, individual types of GVD are useful for addressing other issues. To illustrate the potential of GVDs, two types are considered, chosen because of their implications for GIS.

5.1 Ordinary Voronoi diagram

The ordinary Voronoi diagram (OVD) uses individual points and a Euclidean distance metric to define the tessellation. Formally, suppose that we have a set of n

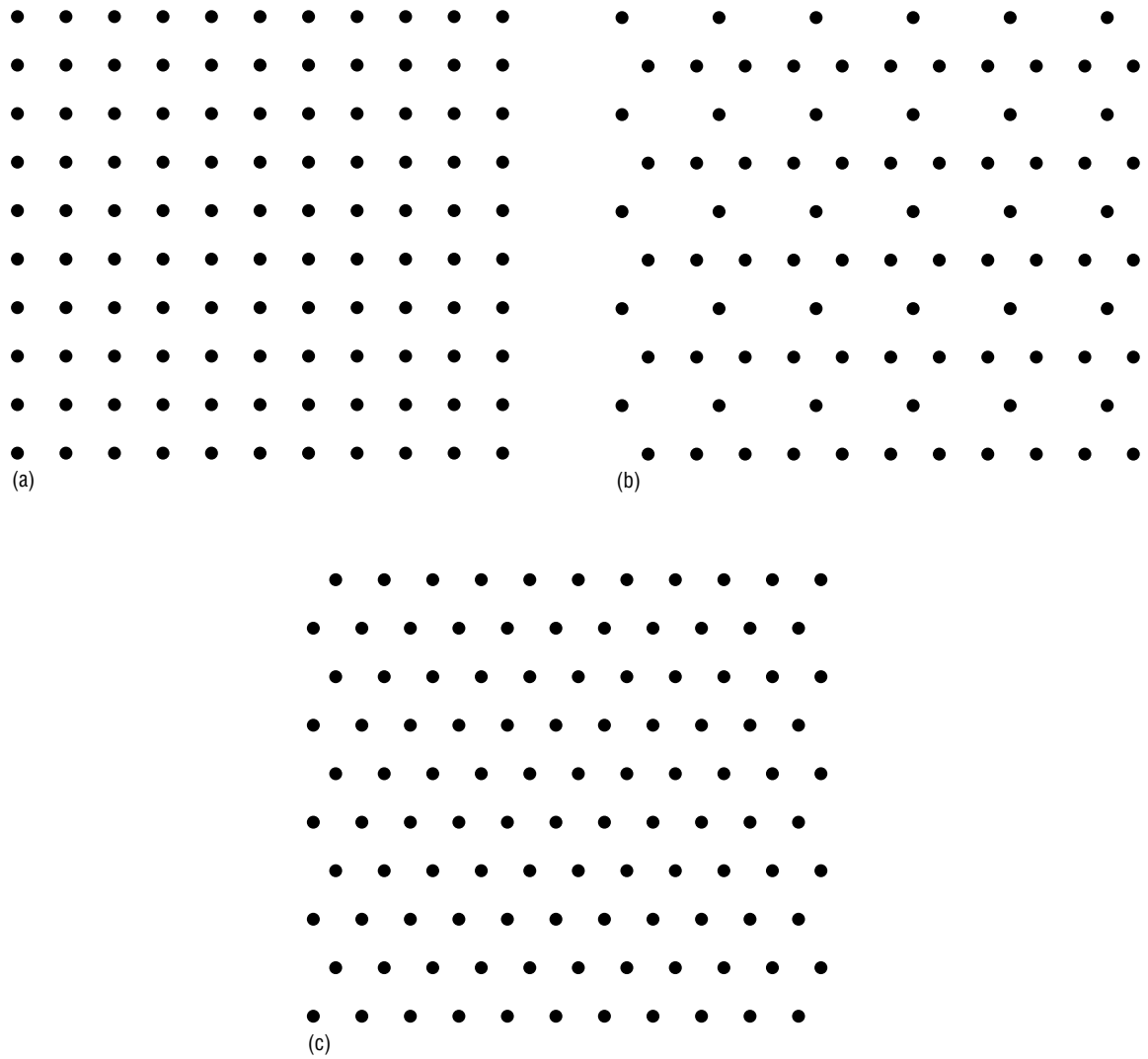

Fig 17. (a) Square, (b) hexagonal, and (c) triangular point lattices.

$(2 \leq n \leq \infty)$ distinct points (generators), $P = \{p_1,...,p_n\}$, located in a finite region S in 2-dimensional space $\Re^2$. To avoid complicated treatment, assume that S is convex. Let $d(p, p_i)$ be Euclidean distance between location p and generator p_i.

We define the region given by:

$$V(p_i) = \{p \mid p \in S;\ d(p, p_i) \leq d(p, p_j),\ j \neq i,\ j=1,...,n\} \quad (12)$$

as the ordinary Voronoi polygon (OVP) associated with p_i and the set given by

$$\upsilon(P) = \{V(p_1),...,\ V(p_n)\} \quad (13)$$

as the OVD of P.

Thus, the interior of $V(p_i)$ consists of all locations in S which are closer to p_i than to any other generator, while the edges and vertices of $V(p_i)$ represent those locations which are equidistant from two or more generators (see Figure 18). Although Voronoi diagrams can be defined for either raster-based or vector-based data structures, the above definition is consistent with the latter. This situation is maintained for all the GVDs discussed here since it permits a more explicit treatment of their topological relationships.

To show how the OVD can be used for locational decision-making, assume that the set of points P in Figure 18 are fire stations and S is a city and that among the questions to be answered are the following:

1 What is the area of the city for which the nearest fire station is the one at p_i?
2 Which is the nearest fire station to a given location p?
3 Which location in the city is farthest from a fire station?

The answer to 1 is given by the OVP of p_i, while 2 is answered by observing which OVP contains p. For example, in Figure 18, p is closest to the station at p_3. Since $V(p_i)$ is a convex polygon, the location in $V(p_i)$ which is farthest from p_i is found in the vertices of $V(p_i)$. These vertices may include those formed by the set of intersections of cell edges with the edges of S, and the set of vertices of S. Define q_{ij} as the jth vertex of $V(p_i)$, $j=1,..., n_i$ where n_i is the number of vertices of $V(p_i)$. Then the farthest location in $V(p_i)$ from p_i is given by the vertex q_i^* of $V(p_i)$ that satisfies

$$d(p_i, q_i^*) = \max\{d(p_i, q_{ij}) \mid j = 1,...,n_i\}. \quad (14)$$

For example, in Figure 18, for $V(p_1)$ this is q_1^*. (3) may be answered by searching for the longest distance among

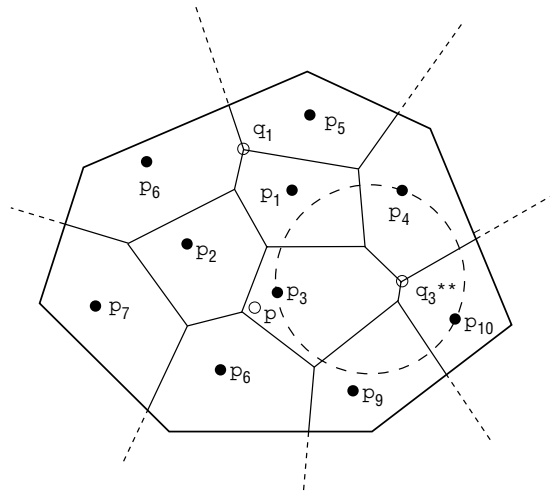

Fig 18. Ordinary Voronoi diagram.

$$\{d(p_i, q_i^*) \mid i = 1,...,n\} \quad (15)$$

or by identifying the vertex q_k** which satisfies

$$d(p_k, q_k^{**}) = \max\{d(p_i, q_i^*) \mid i = 1,...,n\}. \quad (16)$$

In Figure 18, this is the vertex q_3**. Note that q_k** is the centre of a circle radius $d(p_k, q_k^{**})$ (the dashed circle in Figure 18). This circle is the largest circle whose centre is in S and which does not contain any points in P in its interior.

Another fundamental use of the OVD is to define spatial relationships between individual points belonging to a planar point set P such as that defined above. Most work has concentrated on adjacency relationships or the problem of defining a set of neighbours for a given point p_i in P. One solution to this problem is to use the so called 'natural' neighbours of p_i (Sibson 1981) which are those points whose OVPs are adjacent to (p_i) in V(P). For example, in Figure 18 υp_1, p_3, p_6, p_7, and p_8 are the natural neighbours of p_2. This solution has been used in a variety of situations. One involves operationalising spatial models (Besag 1974, 1975; Ord 1975) including spatial autocorrelation models such as Moran's I discussed in section 3. For example, in a study of spatial trends in the grain handling system in the province of Manitoba, Canada from 1943 to 1975, Griffith (1982) set d_{ij} =1 in Equation 8 if two grain handling centres were natural neighbours and d_{ij}=0 otherwise. Another example arises in missing data problems where the unknown value of a variable at a given location must

be estimated from known values at other locations. In their study of rainfall data for Kansas and Nebraska, USA, Haining et al (1984) use natural neighbours to identify which weather stations to use in estimating missing values at other stations.

The missing value problem represents a special case of the more general problem of spatial interpolation (Mitas and Mitasova, Chapter 34). Here there exists a set of n data sites $P=\{p_1,...,p_n\}$, located in (a 2-dimensional) space S, at which the values of some variable z are observed. If it is assumed that these values are observations from a surface defined by z over S, spatial interpolation involves finding a function $f(x)$ which best represents the entire surface and which predicts the values of z for locations other than P. Local interpolants represent the value of the surface $f(x)$ at an arbitrary location p in S as a weighted, usually linear, function of values at nearby data sites, $D(p)$ ($D(p) \subset P$), so that

$$f(x) = \sum_{i=1}^{n_D} w_i z_i,\ p_i \in D(p) \qquad (17)$$

where n_D is the number of nearby sites and w_i is the weight attached to p_i.

There are many ways in which $D(p)$ can be selected (Watson 1992) but one, which also has other advantages described in section 5.2.3, is to use the natural neighbours of p (Gold 1991; Sambridge et al 1995; Sibson 1981; Watson and Philip 1987).

That adjacency relationships for generators are uniquely defined in the OVD (and GVDs, in general) has led Gold (1991, 1992) to propose the GVD as an alternative spatial data model to both the raster and vector ones since it possesses desirable properties of both; a known spatial adjacency structure (raster) and a one-to-one mapping with 'real' map objects (vector).

In terms of spatial relationships, however, the OVD (and GVDs, in general) is not limited to considerations of adjacency. Edwards (1993) and Edwards and Moulin (1995) show that a wide range of linguistic concepts of space such as 'near', 'between', 'among', etc. are amenable to such treatment. For example, suppose there exists a set of fixed reference points, $R_1, ...,R_{10}$ as shown in Figure 19(a) and a displaceable query point Q. Realisation of the relative concepts 'near' and 'far' for Q with respect to the pair of reference points R_1, R_2, can be achieved in the following way. First, define the OVD of the reference points (Figure 19(b)). Next, define the OVD of the reference points plus the query point Q. Figures 19(c) and 19(d) show such OVDs for two different locations of Q. Comparison of Figures 19(c) and 19(d) with Figure 19(b) reveals that the OVP for Q is created by 'stealing' pieces of the OVPs of the reference points (the shaded regions in Figures 19(c) and (d). In Figure 19(c) Q is 'near' to R_1, R_2 and as a result much of its OVP is stolen from the OVPs of these points. In contrast, in Figure 19(d) Q is 'far' from R_1, R_2, so that it steals little of their OVPs. Edwards and Moulin (1995) suggest that the sum of the areas of the regions stolen by Q from R_1, R_2 relative to the area of the OVP of Q may be used as a way of quantifying this notion.

A final use of the OVD is to reconstruct tessellations from incomplete data. For example, in the UK considerable use has been made of the postcode system as a means of georeferencing socio-economic data. However, since no boundaries are defined for unit postcodes, there is a problem reconciling such data with census geography. As a solution, Boyle and Dunn (1991) suggest creating unit postcode zones by defining a Voronoi polygon for each address location contained in the postcode (see Figure 20).

5.2 Higher-order Voronoi diagrams

5.2.1 Order-*k* Voronoi diagram

As with the ordinary Voronoi diagram, begin with a set of points $P = \{p_1, ..., p_n\}$ but now, instead of dealing with individual points, consider subsets of k points selected from P. Although any value of k ($k<n$) may be considered, for simplicity the situation where $k = 2$ is examined, that is, the focus is on pairs of points. The extension to $k>2$ is described by Okabe et al (1992: 142–158).

Let $A^{(2)}(P) = \{P_1^{(2)}, ..., P_i^{(2)}, ..., P_l^{(2)}\}$, where $P_i^{(2)} = \{p_{i1}, p_{i2}\}$, $p_{i1}, p_{i2} \in P$ and $l = {}_nC_2$, be all the possible subsets of P which consist of two points. Let p represent an arbitrary location in the plane and $d(p, p_{ij})$ the Euclidean distance from p to p_{ij}. We define the order-2 Voronoi polygon (O2VP) of $P_i^{(2)}$ as

$$V(P_i^{(2)}) = \{p \mid d(p,p_{i1}) \le d(p,p_j) \text{ and } d(p,p_{i2}) \le d(p,p_j) \text{ for } p_j \in P \backslash P_i^{(2)}\}. \qquad (18)$$

Fig 19. (a) Set of reference points; (b) Ordinary Voronoi diagram of reference points; (c) and (d) Ordinary Voronoi diagram of reference points and query point *Q* for two different locations of *Q*.

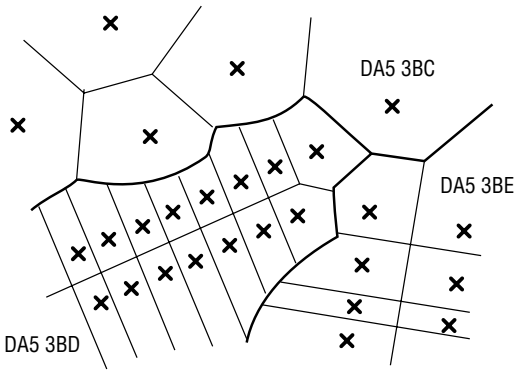

Fig 20. Generating unit postcode boundaries.

Thus, $V(P_i^{(2)})$ consists of all locations for which either p_{i1} or p_{i2} is the first or second nearest point. The set

$$\upsilon\,(A^{(2)}\,(P)) = \upsilon^{(2)} = \{V\,(P_1{}^{(2)}),\ ...,\ V\,(P_l{}^{(2)})\} \qquad (19)$$

is called the order-2 Voronoi diagram (O2VD) generated by P. Figure 21 shows the order-2 Voronoi diagram for the point set in Figure 18.

5.2.2 Ordered, order-*k* Voronoi diagram

In the order-k Voronoi diagram there is no concern with which of the k points in $P_i^{(k)}$ is the nearest, second nearest, ..., or kth nearest. However, in the ordered, order-k Voronoi diagram, this order is considered explicitly. Again, we examine the situation where $k = 2$, that is, for a pair of points. Let $A^{<2>}(P)$ be the set of all ordered pairs of points obtained from the set of points $P = \{p_1, ..., p_n\}$, that is, $A^{<2>}(P) = \{P_1{}^{<2>}, ... , P_i{}^{<2>}, ... , P_l{}^{<2>}\}$ where $P_i{}^{<2>} = (p_{i1}, p_{i2}), p_{i1}, p_{i2} \in P$, and $l = n\,(n-1)$.

Let p be an arbitrary location in the plane and $d(p, p_{ij})$ the Euclidean distance from p to p_{ij}. For a set $P_i^{<2>}$ in $A^{<2>}(P)$, define

$$V(P_i^{<2>}) = \{p \mid d(p,p_{i1}) \le d(p,p_{i2}) \le d(p,p_j),\ p_j \in P\backslash\{p_{i1}, p_{i2}\}\}. \qquad (20)$$

The set $V(P_i^{<2>})$ is called the ordered, order-2 Voronoi polygon (OO2VP) associated with $P_i^{<2>}$. $V(P_i^{<2>})$ consists of all locations for which p_{i1} and p_{i2} are the first and second nearest points, respectively.

The set

$$\upsilon\,(A^{<2>}(P)) = \upsilon^{<2>} = \{V\,(P_1{}^{<2>}),\ ...,\ V\,(P_l{}^{<2>})\} \qquad (21)$$

is called the ordered, order-2 Voronoi diagram (OO2VD) of P. The OO2VD corresponding to the O2VD of Figure 21 is shown in Figure 22.

5.2.3 Applications

As with the ordinary Voronoi diagram, higher order Voronoi diagrams can be used to address locational problems. Once more assume that the points in Figure 18 represent the locations of fire stations in a city. However, this time the possibility

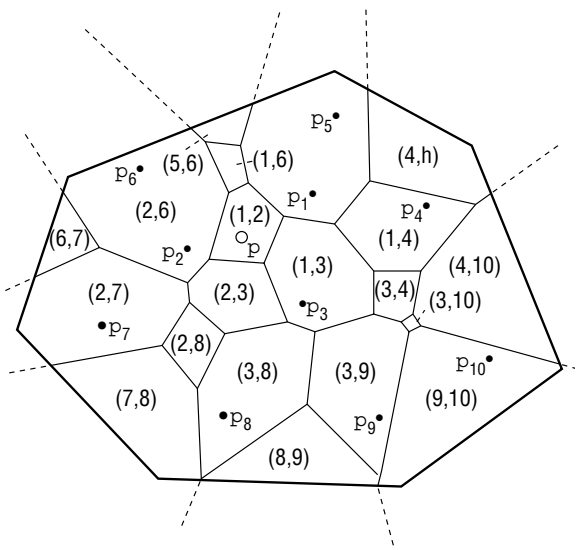

Fig 21. Order-2 Voronoi diagram.

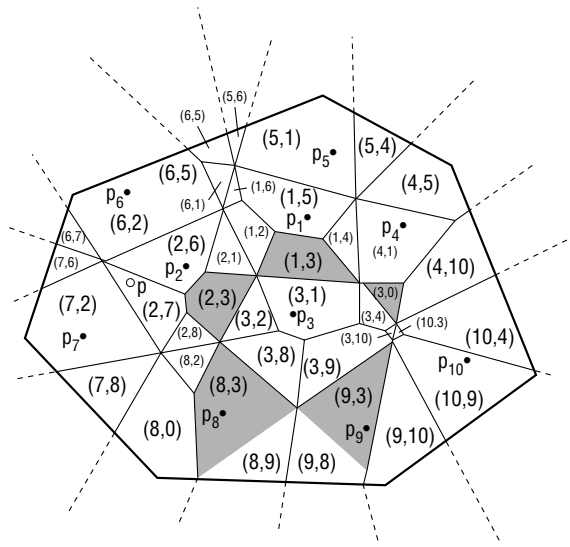

Fig 22. Ordered order-2 Voronoi diagram.

is recognised that, on a given occasion, the equipment at the fire station closest to a given location may already be fully committed, leading to questions such as the following:

1 What are the two closest fire stations to a given location p?
2 What are the first and the second nearest fire stations to a given location p?
3 What is the region of the city for which the station at p_i is the second nearest?

Question 1 may be answered by examining the O2VD of the fire stations and observing in which O2VP the query location p occurs. For example, the two nearest fire stations to p in Figure 21 are those located at p_1, p_2. Questions 2 and 3 require the consideration of the OO2VD of the fire stations. The answer to (2) is found by observing the OO2VP in which p is located (e.g. the first and second nearest fire stations to p in Figure 22 are those at p_2 and p_7, respectively). To answer question 3 we need to find all OO2VPs for which station p_i is the second nearest. The union of these polygons gives the required region (e.g. for the station at p_3 this is the shaded region in Figure 22).

The OO2VD can also be used in spatial interpolation. Recall from the previous section that local interpolants represent the value of a surface $f(x)$ at an arbitrary location p in the plane as a weighted function of the data values at a set of nearby data sites (see Equation 17). It has already seen how natural neighbour relationships can be used to determine the data sites selected. If the ordinary Voronoi diagram is created of the set of data sites $P=\{p_1,..., p_n\}$ plus p, $\mathfrak{V}(P \cup p)$, we know that the OVP of p, $V(p)$, can be exhaustively subdivided into OO2VPs $V((p,p_i))$ (see Figure 23). Following Sibson (1981), if we let $|V((p,p_i))|$ be the area of $V((p,p_i))$, the normalised values $|V((p,p_i))| / \sum |V((p,p_i))|$ can be used as the weights in Equation 17 (see Okabe et al 1992: 347–51 for details). Note that $V((p,p_i))$ can also be considered as the portion of $V(p_i)$ which is stolen by the OVP $V(p)$ created when p is added to P. Thus, the operationalisations of spatial concepts proposed by Edwards and Moulin (1995) and discussed in section 5.1 can also be thought of in terms of OO2VDs.

The area stealing aspect of OO2VPs is also useful in creating maps of nominal scale variables, such as land use, soil or vegetation types, or surficial geology,

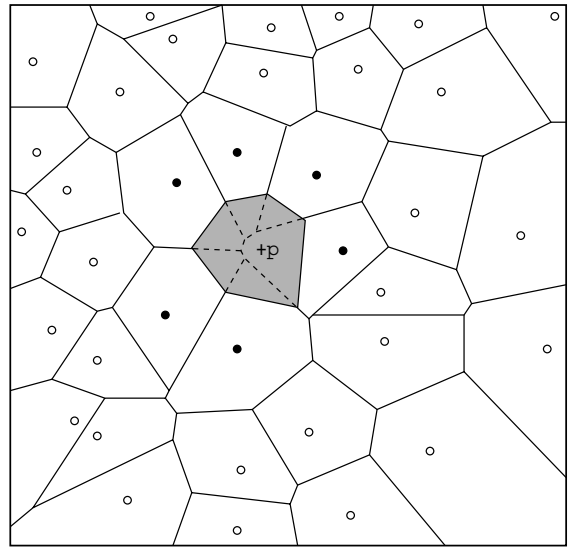

Fig 23. Voronoi diagram ($P \cup p$). Points shown as filled circles are the natural neighbours of p.

from values observed at a set of sampling points $P=\{p_1,...,p_n\}$, especially if we wish to convey the degree of uncertainty involved in the map content (Lowell 1994). Traditional thematic maps are constructed using a Boolean logic which assigns non-sampled locations to one, and only one, class, even though most locations have the possibility of belonging to several different classes. Lowell argues that such situations are better represented by fuzzy maps in which non-sampled locations are assigned fuzzy membership values (FMVs) reflecting the degree of certainty of their belonging to a given class. To generate the FMVs for a given location q, Lowell suggests generating the OVD of the sample points, P, plus q (see Figure 24) and then examining the OO2VPs $V((q,p_i))$. The FMV for a given class x is obtained as the sum of the areas of the $V((q,p_i))$ for which the value at p_i is x, relative to the area of the OVP of q. Thus, in Figure 24, the FMVs for q for classes A, B and C are 0.25, 0.63, and 0.12 respectively.

6 CONCLUSIONS

In GIS, the attention paid to characteristics of different tessellations depends greatly on the context. Typically, such matters receive explicit consideration only when an appropriate spatial data model is being

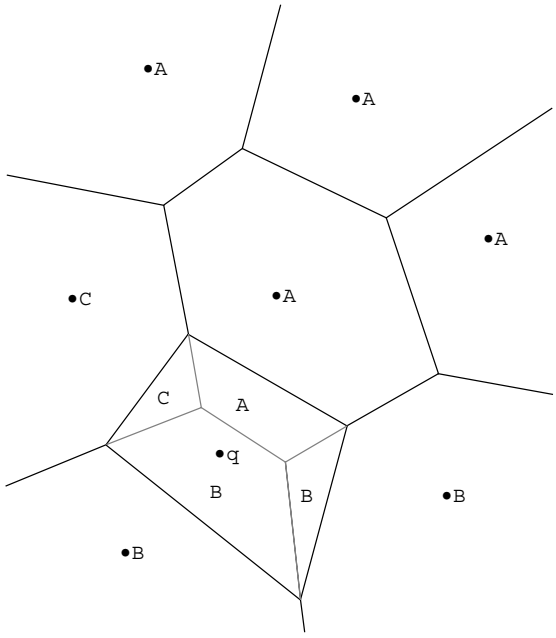

Fig 24. Deriving fuzzy membership values using the ordered order-2 Voronoi diagram.

selected. Once this is accomplished and concerns shift towards analytical issues, tessellation characteristics are rarely considered again. While this chapter reinforces the value of assessing tessellation characteristics in spatial data model selection, it also demonstrates that one should not lose track of them in other contexts. In particular, it is shown by way of examples involving spatial autocorrelation that a tessellation's properties influence the results of analyses of data recorded over the tessellation. Fortunately, staying aware of such properties is not as onerous as might first appear since, as also noted in this chapter, the possible topologic and some metric properties of both regular and irregular tessellations in 2-dimensional space are quite constrained.

Of course, there are many situations in GIS where the objects under consideration do not take the form of tessellations. However, in some of these situations it is possible to generate tessellations from the original objects. Characteristics of these tessellations can then be used to undertake a variety of GIS-related tasks for the original objects. This approach is illustrated by exploring just two of the many members of a family of tessellations known as generalised Voronoi diagrams. Among the tasks which such diagrams can perform are the operationalisation of fundamental spatial concepts such as near, adjacent, and between; spatial interpolation of both nominally- and interval/ratio-scaled variables; and solving locational optimisation problems. While the potential for using tessellations in such roles is already considerable, it is expected to grow further as new forms of tessellations continue to be developed in a number of disciplines interested in various aspects of spatial modelling.

References

Aboav D A 1970 The arrangement of grains in a polycrystal. *Metallography* 3: 383–90

Ahuja N 1983 On approaches to polygonal decomposition for hierarchical image representation. *Computer Vision, Graphics, and Image Processing* 24: 200–14

Ammann R, Grunbaum B, Shephard G C 1992 Aperiodic tiles. *Discrete and Computational Geometry* 8: 1–27

Bell S B M, Diaz B M, Holroyd F C 1989 The HOR quadtree: an optimal structure based on a non-square 4-shape. In Brooks S R (ed.) *Mathematics in remote sensing*. Oxford, Clarendon Press: 315–43

Bell S B M, Diaz B M, Holroyd F C, Jackson M J 1983 Spatially referenced methods of processing raster and vector data. *Image and Vision Computing* 1: 211–20

Bell S B M, Holroyd F C 1991 Tesseral amalgamators and hierarchical tessellations. *Image and Vision Computing* 9: 313–28

Besag J 1974 Spatial interaction and the statistical analysis of lattice systems (with discussion). *Journal of the Royal Statistical Society*, Series B 36: 192–236

Besag J 1975 Statistical analysis of non-lattice data. *The Statistician* 24: 179–96

Boots B N 1979 The topological structure of area patterns: Indian administrative divisions. *The National Geographical Journal of India* 25: 149–53

Boots B N 1980 Packing polygons: some empirical evidence. *The Canadian Geographer* 24: 406–11

Boyle P J, Dunn C E 1991 Redefinition of enumeration district centroids: a test of their accuracy using Thiessen polygons. *Environment and Planning A* 23: 1111–19

Chiu S N 1995 A comment on Rivier's maximum entropy method of statistical crystallography. *Journal of Physics A: Mathematical and General* 28: 607–15

Diaz B M 1986 Tesseral addressing and arithmetic – overview and theory. In Diaz B, Bell S (eds) *Spatial data processing using tesseral methods*. Swindon, National Environment Research Council: 1–10

Ding Y, Fotheringham A S 1992 The integration of spatial analysis and GIS. *Computers, Environment, and Urban Systems* 16: 3–19

Edwards G 1993 The Voronoi model and cultural space: applications to the social sciences and humanities. In Frank A U, Campari I (eds) *Spatial information theory – a theoretical basis for GIS*. Berlin, Springer: 202–14

Edwards G, Moulin B 1995 Towards the simulation of spatial mental images using the Voronoi model. *Proceedings International Joint Conference on Artificial Intelligence (IJCAI-95), Montreal, Canada, 19–26 August*: 63–73

Fotheringham A S, Rogerson P A 1993 GIS and spatial analytical problems. *International Journal of Geographical Information Systems* 7: 3–19

Gold C M 1990 Spatial data structures – the extension from one to two dimensions. In Pau L F (ed.) *Mapping and spatial modelling for navigation*. Berlin, Springer: 11–39

Gold C M 1991 Problems with handling spatial data – the Voronoi approach. *CISM Journal* 45: 65–80

Gold C M 1992 The meaning of 'neighbour'. In Frank A U, Campari I, Formentini U (eds) *Theories and methods of spatio-temporal reasoning in geographic space*. Berlin, Springer: 221–35

Goodchild M F, Haining R P, Wise S 1992 Integrating GIS and spatial data analysis: problems and possibilities. *International Journal of Geographical Information Systems* 6: 407–23

Griffith D A 1982 Dynamic characteristics of spatial economic systems. *Economic Geography* 58: 177–96

Griffith D A 1992 What is spatial autocorrelation? Reflections on the past 25 years of spatial statistics. *L'Espace Geographique* 21: 265–80

Griffith D A 1996b Spatial autocorrelation and eigenfunctions of the geographic weights matrix accompanying geo-referenced data. *The Canadian Geographer* 40: 351–67

Grunbaum B, Shephard G C 1977a Tilings by regular polygons. *Mathematics Magazine* 50: 227–47

Grunbaum B, Shephard G C 1977b The 81 types of isohedral tilings in the plane. *Mathematical Proceedings of the Cambridge Philosophical Society* 82: 177–96

Grunbaum B, Shephard G C 1986 *Tilings and patterns*. New York, W H Freeman & Co.

Haining R P, Griffith D A, Bennett R 1984 A statistical approach to the problem of missing spatial data using a first-order Markov model. *The Professional Geographer* 36: 338–45

Holroyd F, Bell S B M 1992 Raster GIS: models of raster encoding. *Computers and Geosciences* 18: 419–26

Jong P de, Springer C, Veen F van 1984 On extreme values of Moran's *I* and Geary's *c*. *Geographical Analysis* 16: 17–24

Le Caer G, Delannay R 1993 Correlations in topological models of 2D random cellular structures. *Journal of Physics A: Mathematical and General* 26: 3931–54

Lewis F T 1928 The correlation between cell division and the shapes and sizes of prismatic cells in the epidermis of *Cucumis*. *Anatomical Record* 38: 341–76

Lewis F T 1930 A volumetric study of growth and cell division in two types of epithelium – the logitudinally prismatic cells of Tradescantia and the radially prismatic epidermal cells of *Cucumis*. *Anatomical Record* 47: 59–99

Lewis F T 1931 A comparison between the mosaic of polygons in a film of artificial emulsion and in cucumber epidermis and human amnion. *Anatomical Record* 50: 235–65

Lewis F T 1943 The geometry of growth and cell division in epithelial mosaics. *American Journal of Botany* 30: 766–76

Lewis F T 1944 The geometry of growth and cell division in columnar parenchyma. *American Journal of Botany* 31: 619–29

Loeb A L 1976 *Space structures – their harmony and counterpoint*. Reading (USA), Addison-Wesley

Lowell K 1994 A fuzzy surface cartographic representation for forestry based on Voronoi diagram area stealing. *Canadian Journal of Forest Research* 24: 1970–80

Okabe A, Boots B, Sugihara K 1992 *Spatial tessellations: concepts and applications of Voronoi diagrams*. Chichester, John Wiley & Sons

Okabe A, Boots B, Sugihara K 1994 Nearest neighbourhood operations with generalized Voronoi diagrams. *International Journal of Geographical Information Systems* 8: 43–71

Okabe A, Suzuki A 1995 Using Voronoi diagrams. In Dresner Z (ed.) *Facility location: a survey of applications and methods*. New York, Springer: 103–17

Ord J K 1975 Estimation methods for models of spatial interaction. *Journal of the American Statistical Society* 70: 120–6

Perry J N 1995 Spatial analysis by distance indices. *Journal of Animal Ecology* 64: 303–14

Peshkin M A, Strandburg K J, Rivier N 1991 Entropic predictions for cellular networks. *Physical Review Letters* 67: 1803–6

Peuquet D J 1984 A conceptual framework and comparison of spatial data models. *Cartographica* 18: 34–48

Pignol V, Delannay R, Le Caer G 1993 Characterization of topological properties of 2-dimensional cellular structures by image analysis. *Acta Stereologica* 12: 149–54

Rivier N 1985 Statistical crystallography. Structure of random cellular networks. *Philosophical Magazine B* 52: 795–819

Rivier N 1986 Structure of random cellular networks. In Kato Y, Takaki R, Toriwaki J (eds) *Proceedings, First International Symposium for Science on Form*. Tokyo, KTK Scientific: 451–8

Rivier N 1990 Maximum entropy and equations of state for random cellular structures. In Fougere P F (ed.) *Maximum entropy and Bayesian methods*. Dordrecht, Clair: 297–308

Rivier N 1991 Geometry of random packings and froths. In Bideau D, Dodds J A (eds) *Physics of granular media*. New York, Nova Science: 3–25

Rivier N 1993 Order and disorder in packings and froths. In Bideau D, Hansen A (eds) *Disorder and granular media*. Amsterdam, Elsevier Science: 55–102

Rivier N 1994 Maximum entropy for random cellular structures. In Nadal J P, Grassberger P (eds) *From statistical mechanics to statistical inference and back*. Dordrecht, Clair: 77–93

Rivier N, Lissowski A 1982 On the correlation between sizes and shapes of cells in epithelial mosaics. *Journal of Physics A: Mathematical and General* 15: L143–8

Sambridge M, Braun J, McQueen H 1995 Geophysical parameterization and interpolation of irregular data using natural neighbours. *Geophysical Journal International* 122: 837–57

Samet H 1989 *The design and analysis of spatial data structures*. Reading (USA), Addison-Wesley

Sibson R 1981 A brief description of natural neighbour interpolation. In Barnett V (ed.) *Interpreting multivariate data*. New York, John Wiley & Sons Inc. 21–36

Watson D F 1992 *Contouring: a guide to the analysis and display of spatial data*. Oxford, Pergamon Press

Watson D F, Philip G M 1987 Neighbourhood-based interpolation. *Geobyte* 2: 12–16

Zaninetti L 1993 Dynamical Voronoi tessellation IV. The distribution of the asteroids. *Astronomy and Astrophysics* 276: 255–60